

Structure and function of the L-threonine dehydrogenase (TkTDH) from the hyperthermophilic archaeon *Thermococcus kodakaraensis*

A. Bowyer^a, H. Mikolajek^b, J.W. Stuart^a, S.P. Wood^{a,b}, F. Jamil^c, N. Rashid^c, M. Akhtar^{a,c}, J.B. Cooper^{a,b,*}

^a School of Biological Sciences, University of Southampton, Southampton, SO16 7PX, UK

^b Laboratory of Protein Crystallography, Centre for Amyloidosis and Acute Phase Proteins, UCL Department of Medicine (Royal Free Campus), Rowland Hill St., London, NW3 2PF, UK

^c School of Biological Sciences, University of Punjab, Quaid-e-Azam Campus, Lahore 54590, Pakistan

ARTICLE INFO

Article history:

Received 26 February 2009

Received in revised form 21 May 2009

Accepted 12 July 2009

Available online 16 July 2009

Keywords:

Threonine dehydrogenase

X-ray crystallography

Docking

Multi-enzyme complex

Channelling

ABSTRACT

The X-ray structure of the holo-form of L-threonine dehydrogenase (TDH) from *Thermococcus kodakaraensis* (TkTDH) has been determined at 2.4 Å resolution. TDH catalyses the NAD⁺-dependent oxidation of L-threonine to 2-amino-3-ketobutyrate, and is one of the first enzymes in this family to be solved by X-ray crystallography. The enzyme is a homo-tetramer, each monomer consisting of 350 amino acids that form two domains; a catalytic domain and a nicotinamide co-factor (NAD⁺)-binding domain, which contains an α/β Rossmann fold motif. An extended twelve-stranded β -sheet is formed by the association of pairs of monomers in the tetramer. TkTDH shows strong overall structural similarity to TDHs from thermophiles and alcohol dehydrogenases (ADH) from lower life forms, despite low sequence homology, exhibiting the same overall fold of the monomer and assembly of the tetramer. The structure reveals the binding site of the essential co-factor NAD⁺ which is present in all subunits. Docking studies suggest a mode of interaction of TDH with 2-amino-3-ketobutyrate CoA ligase, the subsequent enzyme in the pathway for conversion of threonine to glycine. TDH is known to form a stable functional complex with 2-amino-3-ketobutyrate ligase, most probably to shield an unstable intermediate.

© 2009 Elsevier Inc. All rights reserved.

1. Introduction

Threonine catabolism can be initiated by the following enzymes: threonine aldolase (EC 4.1.2.5), threonine dehydratase (EC 4.2.1.16) and threonine dehydrogenase (TDH; EC 1.1.1.103) (Aronson et al., 1989). Taking these in order, the cytosolic enzyme threonine aldolase catalyses the conversion of threonine to acetaldehyde and glycine but there is much evidence that it has insignificant activity in eukaryotes (Bird and Nunn, 1983; Yeung, 1986) and the human gene is not expressed (Edgar, 2005). The second enzyme, threonine dehydratase, utilises PLP to catalyse the deamination of threonine yielding α -ketobutyrate and ammonia but its activity appeared to be low in a number of mammalian studies (Balleve et al., 1991; Bird and Nunn, 1983). The third enzyme, threonine dehydrogenase (TDH) occurs in the mitochondrial matrix and catalyses the NAD⁺-dependent oxidation of L-threonine to L-2-amino-3-ketobutyrate (Fig. 1), an intermediate in the metabolism of threonine to glycine (Potter et al., 1977). Many studies show that TDH is responsible for the bulk of threonine breakdown in the majority of species (Aronson et al., 1989;

Balleve et al., 1991; Bird and Nunn, 1983; Boylan and Dekker, 1981; Dale, 1978; Davis and Austic, 1997; Hammer et al., 1996; Ray and Ray, 1984) although in animals the threonine dehydratase pathway can become dominant during periods of fasting or high protein diet to mobilise threonine and serine for gluconeogenesis. Hence, it is interesting that in the majority of species there are essentially two enzymes in different cellular compartments that are each capable of assuming a dominant role in threonine catabolism in different metabolic states (Bird and Nunn, 1983).

The product of TDH, 2-amino-3-ketobutyrate, is further cleaved in a co-enzyme A-dependent reaction, catalysed by 2-amino-3-ketobutyrate CoA ligase (KBL), to produce glycine and acetyl-CoA. Overall, this two-step metabolic pathway accounts for 80–100% of threonine catabolised in animal liver (Aoyama and Motokawa, 1981; Balleve et al., 1990; Bird and Nunn, 1983). It has been estimated from studies of hepatic mitochondria that in the fed state 65% of threonine metabolised by TDH is converted to glycine by KBL (Bird and Nunn, 1983; Davis and Austic, 1997). It is likely that the level of CoA determines the flux through the KBL-catalysed reaction and dictates whether threonine is converted to glycine or to the alternative breakdown product aminoacetone (Fig. 1) which is generally produced in relatively small amounts (Davis and Austic, 1997). During fasting, a number of amino acids are sacrificed for gluconeogenesis and threonine is considered to be one of the most important since the increase in its catabolism during

* Corresponding author. Address: Laboratory of Protein Crystallography, Centre for Amyloidosis and Acute Phase Proteins, UCL Department of Medicine (Royal Free Campus), Rowland Hill St., London, NW3 2PF, UK. Fax: +44 (0)207 433 2803.

E-mail address: jbcooper@medsch.ucl.ac.uk (J.B. Cooper).

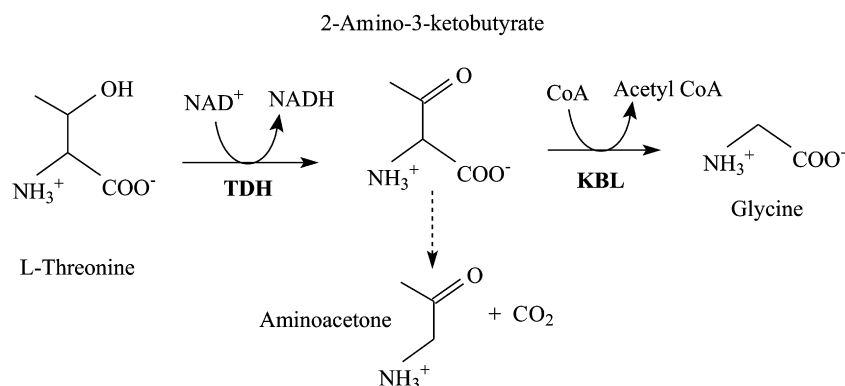


Fig. 1. The reaction catalysed by L-threonine dehydrogenase (TDH) yields 2-amino-3-ketobutyrate, which can either be converted to glycine by ketobutyrate CoA ligase (KBL) or it can decarboxylate to form aminoacetone.

starvation is the third largest of all amino acids and is the largest of the essential amino acids (Balleve et al., 1991).

TDH belongs to the family of oxidoreductases, specifically those acting on the >CHOH group of a donor molecule with NAD⁺ or NADP⁺ as the acceptor (EC 1.1). These enzymes are divided into three classes; the short-chain dehydrogenase family (approximately 250 residues), medium-chain enzymes (350–375 residues) and long-chain dehydrogenases (of greater than 385 residues) (Esposito et al., 2002). It is to the medium-chain family that the 350 amino acid long *T. kodakaraensis* TDH belongs. Typically enzymes in this family contain a catalytic zinc ion co-ordinated by three residues, often two Cys and one His, and a structural zinc-binding site formed by four cysteine residues. Numerous kinetic studies have shown that the reaction proceeds in an ordered manner with NAD⁺ being the first substrate to bind, followed by threonine (Aoyama and Motokawa, 1981; Higashi et al., 2008; Tressel et al., 1986b).

Within the medium-chain dehydrogenase family there exists a high degree of structural similarity between the enzymes, despite their low sequence similarity. However, there are differences in the oligomeric state of the enzymes from higher eukaryotes, which are typically dimeric e.g. horse liver alcohol dehydrogenase (ADH), and those of lower organisms like yeast, bacteria and archaea, which tend to be tetrameric. The majority of TDHs that have been studied are also tetrameric (Tressel et al., 1986b), although a number have been reported to be dimeric (Aoyama and Motokawa, 1981; Kao and Davis, 1994; Wagner and Andreesen, 1995). In the medium-chain dehydrogenase family, the monomers have similar folds comprising two domains; a catalytic domain and a nicotinamide co-factor (NAD⁺)-binding domain, which contains the α/β Rossmann fold characteristic of di-nucleotide-binding proteins (Rossmann and Liljas, 1974). This domain contains a six stranded parallel β -sheet, flanked by α -helices and has the relative strand order of 321456 (Murzin et al., 1995). In dehydrogenases this fold often forms an extended β -sheet between pairs of monomers and in the tetrameric dehydrogenases a small helix α_3 , which binds the structural zinc ion, forms contacts between other pairs of monomers in the tetramer. This can be clearly seen in structures like ADH from *Sulfolobus solfataricus* (SsADH) (Esposito et al., 2002), ADH from *Saccharomyces cerevisiae* (ScADH) (Leskovac et al., 1976) and TDH from *Pyrococcus horikoshii* (PhTDH) (Ishikawa et al., 2007).

It has been reported that the product of TDH, 2-amino-3-ketobutyrate, is highly unstable with a half-life of less than one minute due to its spontaneous breakdown to aminoacetone (Laver et al., 1959). It has been shown that the conversion of threonine to glycine by the pathway shown in Fig. 1 requires the formation of a complex between TDH and KBL since when both enzymes are physically separated, e.g. by a dialysis membrane, threonine is converted instead to

aminoacetone and CO₂ (Tressel et al., 1986b). Experiments using mixtures of TDH and KBL showed that increasing the concentration of KBL reduced the amount of aminoacetone produced and increased the production of glycine. In more recent studies, it has been claimed that in the absence of KBL, TDH actually catalyses an oxidative decarboxylation of threonine to aminoacetone with no 2-amino 3-ketobutyrate acid being produced (Tressel et al., 1986b). The enzyme is inhibited by bicarbonate and aminoacetone suggesting that these are *bona fide* reaction products. In addition, prokaryotic TDH is also recognised as an important enzyme in vitamin B₁₂ biosynthesis since aminoacetone is used to form the aminopropanol side group of this co-factor (Roth et al., 1996).

Intriguingly it has been observed that mammalian TDH and KBL (both mitochondrial matrix enzymes) co-elute on gel-filtration with an apparent molecular mass of 150 kDa, which is consistent with the formation of a stable complex of 2 KBL dimers with 1 TDH tetramer (Tressel et al., 1986b). Accordingly the *Escherichia coli* genes for KBL and TDH are within the same operon and are transcribed from a common promoter (Aronson et al., 1989). Fluorescence studies showed that the TDH–KBL complex has a dissociation constant of 5–10 nM and a stoichiometry in accord with the gel-filtration measurements. Thus the TDH–KBL complex appears to be a specific interaction that prevents the enzymatic or spontaneous decarboxylation of the product of TDH, 2-amino-3-ketobutyrate to aminoacetone. Most procedures for purification of mammalian TDH or KBL involve sonication of liver mitochondria, which disrupts the complex and accordingly the sonicated extracts convert threonine predominantly to aminoacetone. However when purified KBL is added to TDH, glycine is produced from threonine. The nature of substrate channelling between these two enzymes remains to be established and the possibilities include a micro-compartment or tunnel through which the product of TDH passes to KBL or direct transfer between the active sites. Interestingly the complex in *E. coli* is capable of catalysing the reverse reaction i.e. the synthesis of threonine from glycine, but this process is about 50 times less efficient than the forward reaction (Marcus and Dekker, 1993). The inefficiency of threonine biosynthesis by the reverse reaction is also consistent with the essentiality of threonine in the diet of mammals.

Following completion of the human genome, the gene for TDH was initially elusive but it was eventually located at 8p23-22 by homology with the known mammalian TDH sequences (Edgar, 2002a, 2002b). Intriguingly the human gene possesses three mutations, two of which disrupt splicing of the transcript and the third introduces a premature stop codon, thus giving rise to truncated proteins of 157 and 230 amino acids which lack large parts of the co-factor binding domain and the entire catalytic domain (Edgar, 2002b). Since the human TDH gene is expressed it is classed

as an 'expressed pseudogene' (Edgar, 2002b) and the lack of any hereditary diseases linked with defects in TDH or KBL suggests that the alternative pathway of threonine catabolism initiated by threonine dehydratase is dominant in this species. Nonetheless this suggests that TDH is an excellent target for drug development since many parasites and other pathogens depend on functional TDH enzyme.

A number of TDHs have been structurally characterised, including the enzymes from *P. horikoshii* (Ishikawa et al., 2007), *Thermus thermophilus* and *Flavobacterium frigidimaris* (PDB codes 2DFV, 2EJV and 2YY7 respectively). Here we report the crystal structure of TkTDH from *Thermococcus kodakaraensis*, which has been solved at a resolution of 2.4 Å revealing the detailed tertiary fold and quaternary structure of the molecule. Analysis suggests that the biologically active form of the molecule is a tetramer, in agreement with ADHs from lower life forms. The co-factor NAD⁺ is well defined by the electron density map for each subunit, thus identifying the active site. The structure has been used to model the multi-enzyme complex that TDH forms with KBL, suggesting how two molecules of the dimeric KBL enzyme can simultaneously bind to one tetramer of TDH and thus permit channelling of an unstable intermediate between the active sites of both enzymes.

2. Materials and methods

2.1. Expression and purification

The expression and purification of TkTDH was carried out according to the methods previously described in Bowyer et al. (2008) and Bashir et al. (2009). Recombinant pET-tdh plasmid was transformed and expressed in *E. coli* BL21 (DE3). Gene expression was induced at mid-log phase with 0.2 mM IPTG at 37 °C. The resulting TkTDH protein was soluble and was purified by sonication, heating of the cell lysate, anion exchange and hydrophobic interaction chromatography. The purified enzyme was found to have a subunit molecular mass of 38,016 Da by electrospray mass spectrometry and gel-filtration indicated that the biologically active molecule was tetrameric.

2.2. Crystallisation and data collection

Crystallisation conditions were screened at room temperature using the hanging-drop vapour diffusion method on 24-well plates. Both Molecular Dimensions screens MD 1+2 and Jena Biosciences JB screens 1–10 were used and a suitable condition was identified (MD2 29). Three rounds of optimisation screens were set up to refine the conditions, as frequently it was found that fractured crystals formed, leading to twinned diffraction data that proved too difficult to process. 5% (v/v) glycerol was added to the final round of optimisation and single crystals of TkTDH eventually grew in 0.05 M sodium citrate pH 5.6, 2.4 M ammonium sulphate, 0.1 M sodium/potassium tartrate, 0.1 mM ZnCl₂ and 5% (v/v) glycerol. Crystals were transferred to mother liquor solution containing 10% glycerol as cryoprotectant and frozen in a cryostream at 100 K and stored in liquid nitrogen. They were then taken to the European Radiation Synchrotron Facility (ESRF) in Grenoble, France, where a dataset was collected to 2.4 Å resolution using beam line ID14-3. One-hundred and ninety images were collected with 1° oscillations and an exposure time of 30 s per image with three passes per image.

2.3. Structure determination and refinement

The data were processed using MOSFLM (Leslie, 2006; CCP4, 1994), SCALA (Evans, 2006) and other programs in the CCP4 suite

(CCP4, 1994) in space group *P*₄₃₂₁₂ which gave an *R*_{merge} of 0.148. The unit cell dimensions of *a* = *b* = 124.5 Å, *c* = 271.1 Å correspond to an estimated solvent content of 64.9% (v/v) and *V*_M = 3.5 Å³/Da for a tetramer in the asymmetric unit. A 5% free *R*-flag data set was picked in thin shells using DATAMAN (Kleywegt and Jones, 1996). Molecular replacement was performed using one monomer of PhTDH (PDB code 2DFV) as a model in PHASER (Qian et al., 2007) and gave a log likelihood gain (LLG) of 15485 for *P*₄₃₂₁₂, (after rigid-body refinement), which was significantly higher than that for any of the other space groups in the 422 point group (the next best solution for *P*₄₃₂₁₂ had a LLG of 780).

Refinement was initially carried out, with data to a resolution of 2.4 Å, using CNS (Brunger, 2007). Three rounds of simulated annealing up to 4000 °C and rigid-body refinement with tight NCS restraints between the four subunits, interspersed with model building in COOT (Emsley and Cowtan, 2007), were carried out. During the third round, group *B*-factors were also refined. Two rounds of rigid-body refinement were then carried out using PHENIX (Adams et al., 2002) with several cycles of tight NCS restraints, lower temperature simulated annealing and translational symmetry restraints, again interspersed with model building. The final seven rounds of refinement were carried out using REFMAC (CCP4, 1994), initially with medium NCS restraints applied, although these were not used in the final rounds. A total of 490 water molecules were added during the rebuilds and the co-factor NAD⁺ was built into the electron density using COOT and the structure rebuilt using both the 2*F*_o–*F*_c and *F*_o–*F*_c maps. The NAD⁺ co-factor was refined with 50% occupancy since this value gave best agreement with difference maps. The final *R*_{factor} and *R*_{free} values are 22.0% and 27.6%, respectively, and the diffraction data and crystallographic refinement statistics are summarised in Table 1. The figures of the structure were prepared using Pymol (DeLano, 2002). Areaimol (CCP4, 1994) was used to calculate the surface area for an individual monomer, a dimer and the biological tetrameric protein. Buried surface areas were calculated using CNS (Brunger et al., 1998), and COOT (Emsley and Cowtan, 2007) and TURBO-FRODO (BioGraphics, Marseille) were used to generate RMS deviations and align subunits. ALSCRIPT (Barton, 1993) was used to colour-code the primary sequence alignment. The structure and diffraction data have been deposited in the Protein Databank with PDB ZD: 3GFB.

2.4. Docking

To model the TDH–KBL multi-enzyme complex, docking was performed using HADDOCK2.0 webserver (de Vries et al., 2007)

Table 1

Refinement statistics for native TkTDH. Values in parenthesis are for the outer resolution shell.

Resolution range (Å)	73.9–2.4 (2.5–2.4)
Space group	<i>P</i> ₄ ₃ ₂ ₁ ₂
<i>R</i> _{factor} (%)	22.0
<i>R</i> _{free} (%)	27.6
Subunits per asymmetric unit	4
Number of non-hydrogen protein atoms	10672
Number of water molecules	490
Wilson's B-factor (Å ²)	42.6
Average B-factor (Å ²)	43.0
RMSD bond lengths (Å)	0.038
RMSD bond angles (deg.)	2.968
Matthew's coefficient (Å ³ /Da)	3.50
Solvent content (%)	64.90
<i>R</i> _{merge} (%)	14.6 (59.0)
Completeness (%)	100 (100)
Average <i>I</i> /σ	14.8 (2.7)
Multiplicity	14.5 (11.8)

* $R_{\text{merge}} = \sum_{\text{hi}} |I_{\text{hi}} - I_{\text{h}}| / \sum_{\text{hi}} I_{\text{hi}}$ where *I*_h is the mean intensity of the scaled observations *I*_{hi}.

which allows for flexible protein-protein docking. The starting structures used were the *E. coli* KBL structure (PDB ID: 1FC4) (Schmidt et al., 2001) and TDH presented in this paper. To limit computational overhead only one half of TDH, consisting of chains A and B, was used with residues selected to bias the docking away from the surface involving TDH tetramer formation. The default protocol was used which employs three stages, (1) 1000 rigid-body docking solutions are generated with random orientations and energy minimised, (2) the 200 best solutions based on intermolecular energies are subjected to simulated annealing in torsion angle space and (3) further refinement in Cartesian space in explicit water. During the final two stages selected surface residues were allowed to move. The final structures are grouped based on a pairwise backbone rmsd matrix using the clustering algorithm described in Daura et al. (1999).

3. Results

3.1. Primary structure similarity

TkTDH possesses 350 amino acid residues and has a molecular mass of 38,016 Da per monomer, as determined by electrospray mass spectrometry (Bowyer et al., 2008). As well as displaying high sequence similarity with other TDHs from hyperthermophiles (e.g. *Pyrococcus abyssi* TDH has 88%, *P. furiosus* 88% and *P. horikoshii* 87%), TkTDH is homologous to other TDHs and some ADHs, as shown in Fig. 2. In the alignment there are some highly conserved residues, most notably the four cysteine residues that co-ordinate the structural zinc ion (Cys97, Cys100, Cys103 and Cys111), the four residues proposed to co-ordinate a catalytic zinc ion (Cys42, His67, Glu68 and Glu152) and the GxGxxG NAD⁺ binding motif (formed by Gly175, Gly177 and Gly180). Of the residues co-ordinating the catalytic zinc ion, the first three are conserved between TDHs and ADHs, whereas the fourth residue Glu152 is more variable e.g. in *E. coli* ADH (EcADH) this residue is an Asp and in *Aeropyrum pernix* ADH (ApADH) it is alanine. The structural zinc-binding region of TkTDH contains four cysteine residues ⁹⁷CGKCYACKHNRYHVC¹¹¹ and shows four differences from the TDH's of other hyperthermophiles. There are further differences from the mesophilic homologues where this loop is generally more polar, as shown in Fig. 2.

3.2. Structure of the monomer

Each monomer of TkTDH is folded into two domains; a catalytic domain (residues 153–292) and a nicotinamide co-factor (NAD⁺)-binding domain (residues 3–152 and 293–349), which adopts a classical α/β Rossmann fold motif, characteristic of di-nucleotide-binding proteins. In total the monomer contains 12 α -helices and 16 β -strands, making up 31% and 23% of the structure, respectively. The overall tertiary structure of the monomer with the bound NAD⁺ is shown in Fig. 3 along with the overall topology. The secondary structure labelling in Fig. 3 is based on the nomenclature for ADHs as described by Korkhin et al. (1998). The five helices (B–E and 3₁₀S) and seven β -strands (A–F and S) from residues 171 to 290 form the α/β Rossmann fold of the co-factor binding domain. Six of these β -strands make a parallel β -pleated sheet flanked by the five helices and the seventh β -strand. The catalytic domain consists of a core of mostly anti-parallel β -strands (1–9) with seven α -helices (1–7) at the surface of the molecule.

In each monomer, there is a short α 3 helix within a protruding lobe region which contains the four conserved cysteines that co-ordinate the structural zinc ion with tetrahedral geometry in PhTDH (Ishikawa et al., 2007). It is thought this region, which plays an important role in quaternary contacts, may confer further

thermostability on the enzyme (Morikawa et al., 1994; Itoh et al., 2003), although it is present in some mesophilic medium-chain dehydrogenases. However, this region appears disordered in the TkTDH structure, although it is expected that in the presence of a bound Zn²⁺ ion it would be more ordered. Nearby there is a long 18 residue α 5 helix (residues 145–162), the longest in the molecule, which forms a linker between the two domains, possibly acting as a hinge when NAD⁺ and threonine bind. This helix is well defined in the electron density map and is clearly kinked at Glu151, indicating a possible bending effect exerted by the catalytic metal ion which is held by the adjacent residue Glu 152.

Three *cis*-peptide bonds are observed in the structure preceding Pro62, Pro194 and Trp297. Pro62 is highly conserved amongst both TDHs and ADHs, as is the *cis*-peptide conformation that it adopts in the tertiary structure. However, both Pro194 and Trp297 appear to only be conserved in TDHs, and not in ADHs. Trp297, a rare non-prolyl *cis*-peptide, is located on the surface of the catalytic domain of both TkTDH and PhTDH where it appears to form part of a hydrophobic cluster with Trp137, Trp300 and Tyr301. The electron density for this region including the *cis*-peptide itself is very well defined in both structures. All four of these hydrophobic residues appear to be conserved amongst TDHs from hyperthermophiles, suggesting this cluster may be a contributing factor to their thermostability. However, it is not always present in ADHs from hyperthermophiles and in some mesophilic ADHs alternative hydrophobic residues are present and form a similar cluster.

The fold of the TkTDH monomer is similar to that of *P. horikoshii* TDH and both enzymes have similar topology to the medium-chain ADHs from mesophilic organisms, as illustrated in Fig. 4. TkTDH superimposes with PhTDH with an RMS deviation of less than 0.57 Å for all 348 C- α carbon atoms and it superimposes with SsADH with an RMS deviation of 1.90 Å for 300 C- α atoms closer than 3.5 Å, reflecting the lower sequence identity in the latter comparison.

3.3. Structure of the tetramer

TkTDH adopts a homo-tetrameric structure within the crystallographic asymmetric unit, shown in Fig. 5, and this is likely to be the biologically active form of the enzyme, in keeping with many medium-chain dehydrogenases of lower organisms. The tetramer structure is very similar to that of PhTDH (with an RMS deviation of 1.06 Å for all four subunits) and, despite low levels of sequence identity, is quite similar structurally to SsADH which has 28.5% identity and ScADH which has 25.9% identity. Essentially the quaternary structure comprises a dimer of dimers. The dimers formed by monomers A and B (and C and D) bury 1552.6 Å² of the 15,425.4 Å² accessible surface per monomer, resulting in a solvent-accessible surface area of 27,287.8 Å² for each dimer. Association of the dimers into a tetramer buries a further 5,038.9 Å² giving a total accessible surface area of 50,168.9 Å². Figures similar to these were found for PhTDH (Ishikawa et al., 2007). As has been found in many ADHs and PhTDH, the β -strands of the Rossmann fold form an extended 12-stranded β -sheet across the dimer interface to create an extensive region of contact between monomers A and B (and C and D). This binding involves β -strands F (residues 273–275) and S (residues 287–290) of both subunits, where the β F strand of monomer A forms hydrogen-bonds with the anti-parallel β F strand of monomer B, and likewise β S of monomer A hydrogen-bonds the anti-parallel β S of monomer B. In addition, there is a minor interaction at the structural lobe loop involving helix α 3 (95–117) where hydrogen bonds and electrostatic interactions bridge the two dimers to form the tetramer. This interaction buries 1172.1 Å² accessible surface area between each monomer in the following pairings of A/C and B/D. Additional pairings of monomers A with D and B with C arise from interactions between helices α B

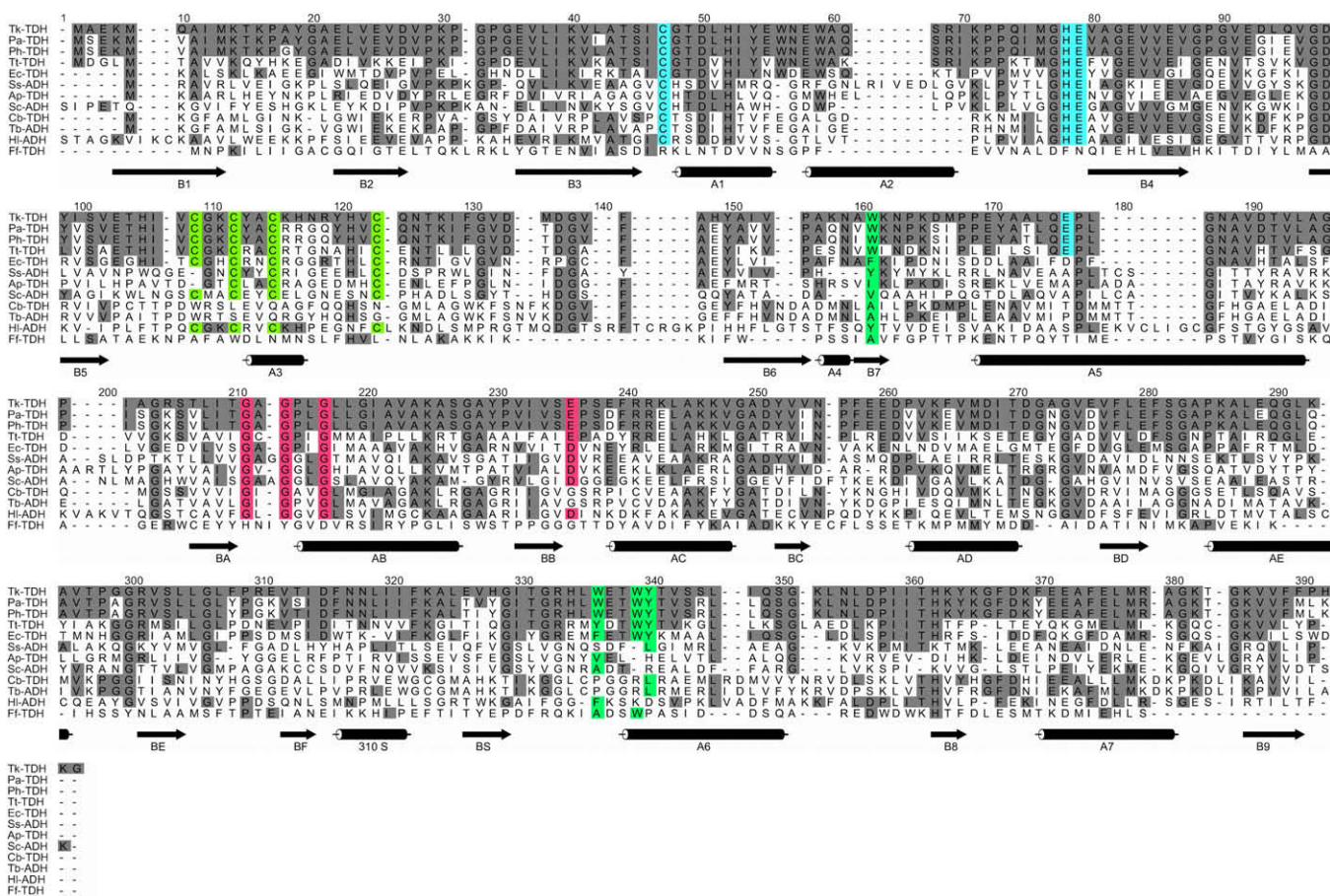


Fig. 2. An amino acid sequence alignment comparing TKTdH with other TDHs and ADHs from a variety of other organisms. TKTdH displays 87.4% sequence identity with PhTdh (*Pyrococcus horikoshii*), 87.6% identity with PaTdh (*Pyrococcus abyssi*), 51.0% identity with TtTdh (*Thermoanaerobacter tengcongensis*), 42.8% identity with EcTdh (*Escherichia coli*), 26.3% identity with HiAdh (Horse Liver ADH), 28.5% identity with SsAdh (*Sulfolobus solfataricus*), 26.9% identity with CbAdh (*Clostridium beijerinckii*), 24.9% identity with TbAdh (*Thermoanaerobacter brockii*), 26.7% identity with ApAdh (*Aeropyrum pernix*), 25.9% identity with ScAdh (*Saccharomyces cerevisiae*) and 9.6% identity with FtAdh (*Flavobacterium frigidimaris*). The conserved cysteine residues thought to co-ordinate the structural zinc ion are shown in bright green, the conserved Cys and His and Glu residues thought to co-ordinate the catalytic zinc ion are shown in bright blue and the conserved GxGxxG NAD⁺ binding motif is shown in pink. The four hydrophobic residues that form a cluster in some medium-chain dehydrogenases are shown in light green. The α -helical and β -strand secondary structure is shown diagrammatically beneath the sequences. (For interpretation of colour mentioned in this figure legend the reader is referred to the web version of the article.)

and $\alpha 6$. Specifically Gly168 in the loop between $\alpha 5$ and βA of monomer A forms two hydrogen-bonds with Ser 305 ($\alpha 6$) of monomer D while Gly191 (αB) of monomer A hydrogen-bonds with Ala189 (αB) of monomer D. The A/D and B/C interface buries 1150.4 Å² of solvent-accessible surface area of each monomer. The relatively small areas buried by these additional dimer contacts, compared with that buried by the main A/B and C/D dimer contact regions justifies the description of this enzyme as a dimer of dimers.

3.4. Structural zinc-binding site

Most medium-chain dehydrogenases contain a catalytic zinc ion and a structural zinc ion located in the lobe loop of the catalytic domain where it most likely rigidifies part of the protein that is important in quaternary contacts (Jelokova et al., 1994). Likewise in TKTdH, a structural zinc ion was expected to bind in the lobe loop region, although this was not observed in the crystal structure. However, the zinc content does vary between ADHs with either one or two zinc ions being present per subunit, for example *Thermoanaerobacter brockii* ADH (TbADH) contains only a catalytic zinc ion (Bogin et al., 1997) whereas EcADH contains both a catalytic and structural zinc ion (Sulzenbacher et al., 2004). The importance of the structural zinc ion has been demonstrated with mammalian ADH by site-directed mutagenesis of the four co-ordinating cysteine residues which gave inactive, unstable enzyme that

was unable to ligate zinc (Ishikawa et al., 2007). However the structural zinc ion is not present in ADHs from some organisms such as *T. brockii* (Bogin et al., 1997) and *Clostridium beijerinckii* (Korkhin et al., 1998). Although catalytically active TKTdH was used in the crystallisation trials, no electron density was observed for zinc ions in the structure, despite Zn²⁺ being present in the mother liquor. One possible explanation is that citrate anions in the crystallisation buffer may have chelated any zinc ions present in the protein. Citrate is frequently used to solubilise zinc ions in crystallisations since it has a high binding constant for this metal ion of almost 10⁵ M⁻¹ (Smith and Martell, 1976). Hence it is conceivable that it may effectively remove Zn²⁺ from solvent-accessible sites in the protein. In the TKTdH structure it was also observed that the 'lobe loop' region (97–115) exhibited highly disordered electron density and proved difficult to model, indicating that the structural zinc is indeed required to stabilise the loop, as suggested for PhTdh (Ishikawa et al., 2007). It was however observed that the four conserved cysteine residues (Cys97, Cys100, Cys103 and Cys111) did co-localise to a central position large enough to accommodate a zinc ion with tetrahedral geometry without disrupting other residues. Mammalian ADHs, although most commonly dimeric, do usually contain both catalytic and structural zinc ions, whereas some bacterial ADHs adopting a tetrameric structure lack the structural zinc ion, suggesting that any correlation between the presence of a structural zinc in the lobe loop

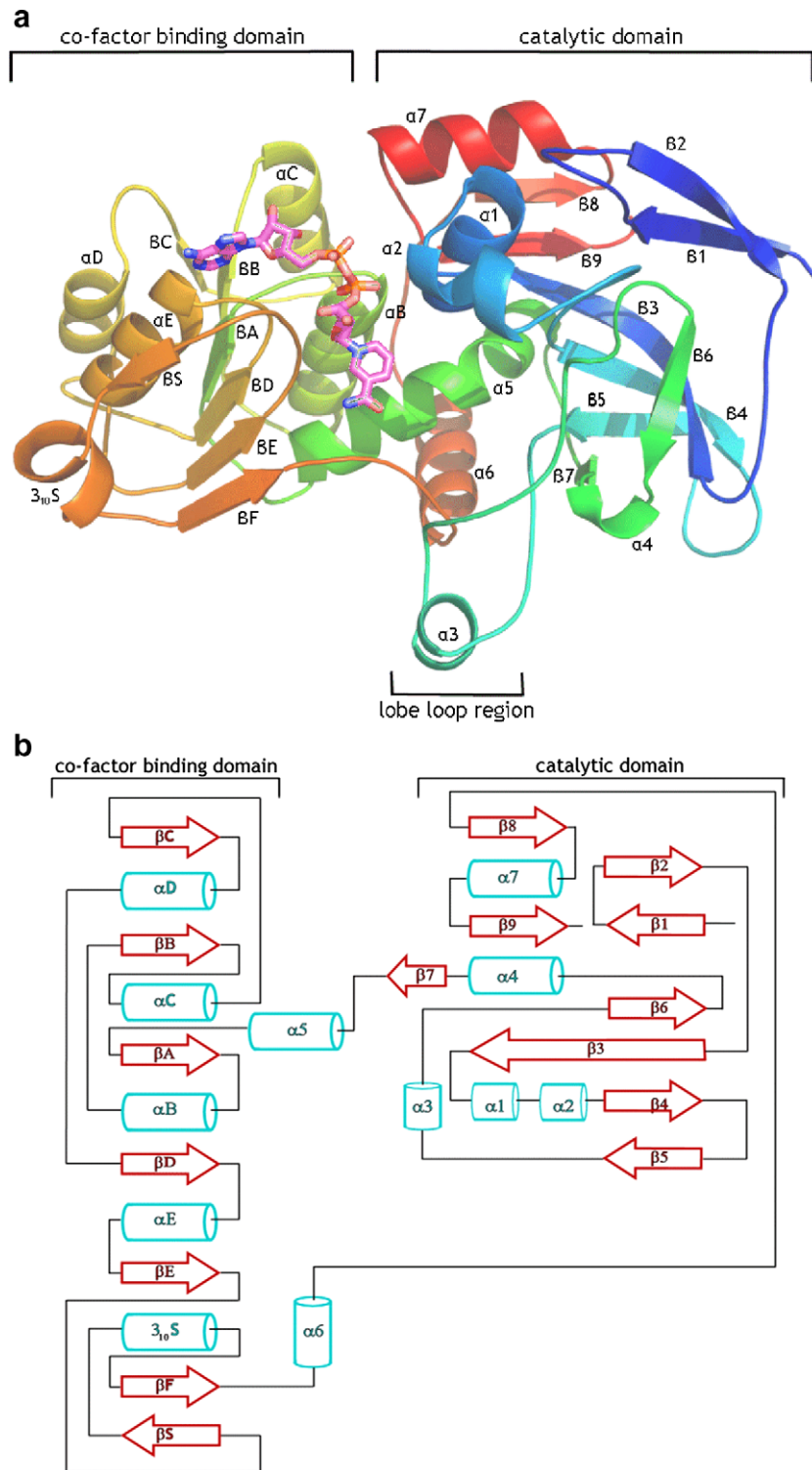


Fig. 3. (a) A ribbon diagram of a monomer of TkTDH. Helices 1–4, 6 and 7 and β -strands 1–9 comprise the catalytic domain, helices B–E and 3_{10} S and β -strands A–F and S form the NAD^+ -binding domain and helix 5 acts as a linker between the two. (b) The overall topology with α -helical segments shown in blue and β -strands shown in red. The five α -helices (B–E and 3_{10} S) and seven β -strands (A–F and S) from residues 171–290 form the α/β Rossmann fold of the co-factor binding domain.

region, and the oligomeric state of the enzyme is not straightforward.

3.5. Active site

The catalytic and NAD^+ co-factor binding domains are linked by helix $\alpha 5$ which, along with residues 290–298, form a large cleft, the

shape of which is indicated in Fig. 6(a). The cleft is large enough to accommodate both the NAD^+ co-factor and threonine substrate. In ADHs the active site possesses a catalytic zinc ion and although this is present in PhTDH, it was absent from the TkTDH structure. However, as already discussed, the absence of zinc in TkTDH could be due to its chelation by citrate in the crystallisation conditions. Although a catalytic zinc ion is absent from the TkTDH structure,



Fig. 4. A ribbon diagram showing a monomer of TkTDH (red) aligned with monomers of PhTDH (pink) and SsADH (green). The close similarity of the TkTDH and PhTDH structures, which have 87% sequence identity, is reflected in the RMS deviation of 0.57 Å for all 348 C α 's. TkTDH superimposes with SsADH (29% sequence similarity) with an RMS deviation on 1.90 Å for 300 C α carbon atoms that are closer than 3.5 Å. (For interpretation of colour mentioned in this figure legend the reader is referred to the web version of the article.)

the four conserved residues postulated to co-ordinate it (Cys42, His67, Glu68 and Glu152) are in an arrangement that would appear to be capable of ligating a central zinc ion.

Electron density was observed in the co-factor-binding domain for NAD⁺ and is shown in Fig. 6(b). It is thought that the binding of NAD⁺ to TDH causes a conformational change in which residues of the active site cleft are brought closer together, thereby enabling threonine to bind and the reaction to occur (Ishikawa et al., 2007). This ordered Bi Bi mechanism of binding is supported by studies of PhTDH (Higashi et al., 2008), chicken liver TDH (Aoyama and Motokawa, 1981) and mammalian TDH (Tressel et al., 1986b). The binding of threonine is thought to cause a further rearrangement of the α 1 helix into a closed conformation, bringing it closer to the active site, as observed in horse liver ADH (HIADH) (LeBrun et al., 2004; Ramaswamy et al., 1999). The unstable product 2-amino-3-ketobutyrate leaves the enzyme active site prior to the release of NADH.

In ThTDH the NAD⁺ co-factor occupies the active site pocket and is bound predominantly by Van der Waal interactions and hydrogen bonds with the surrounding amino acid residues, shown in Fig. 6(c). The distance between the nicotinamide of NAD⁺ and the putative zinc site is approximately 7 Å which is sufficient to accommodate the threonine substrate. The main chain of Leu179 forms two hydrogen bonds, one with the nicotinamide ring and the other with an oxygen of the first phosphate group. The nicotinamide ring is also hydrogen-bonded by the main chains of Leu266 and Ile291, with many contacts also being formed with Asn156 and Gly267. The nicotinamide ring was observed to bind in a single conformation, unlike PhTDH where two alternative conformations were observed with equal occupancy (Ishikawa et al., 2007). The main chain of Leu268 binds an oxygen of the first ribose ring and

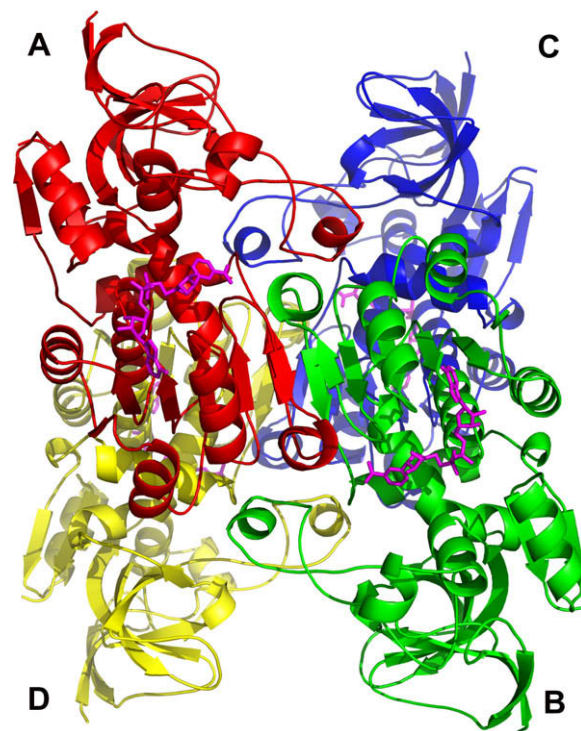


Fig. 5. The tetrameric structure of TkTDH emphasising its 'dimer of dimers' quaternary structure and showing the co-factor NAD⁺ bound to each subunit. Monomer A is shown in red, B in green, C in blue and D in yellow. The overall fold of the enzyme is dominated by the extended β -sheet formed by the Rossmann fold of monomers A and B in the foreground (and by that of subunits C and D in the background). (For interpretation of colour mentioned in this figure legend the reader is referred to the web version of the article.)

makes many other contacts. The second phosphate makes contacts with Pro178 and Arg204, the second of which also hydrogen-bonds an oxygen of the second ribose ring. A second hydrogen bond is made with this ribose ring by Glu199 and many contacts are made by the ribose with Gly175 and Phe243. Arg204 is highly conserved amongst TDHs but not ADHs, whereas Glu199 is present in both TDHs and ADHs. Kinetic parameters have been measured for mutants of PhTDH, in which Glu199 and Arg204 were mutated to Ala, and the results indicated that these residues were indeed very important for NAD⁺ binding (Ishikawa et al., 2007). The adenosine ring is hydrogen bonded to Ser198, as well as making significant contacts with Pro200. A significant effect of these binding contacts is that the nicotinamide ring is bound in a slot formed by Leu179, Leu266 and Leu268 and the adenine ring is held by hydrogen bonds with Ser198 and two water molecules.

A number of other hydrogen bonds are formed between the co-factor NAD⁺ and water molecules at the active site, including one found to be conserved at this site in other di-nucleotide binding proteins containing a Rossmann fold (Bottoms et al., 2002). In TkTDH a total of eight water molecules have been found to directly hydrogen-bond with NAD⁺ along its length, most of which form further bonds with either residues or other water molecules. One of these waters is strongly conserved and binds the co-factor and three protein residues. As can be seen in Fig. 6(c), it forms four hydrogen bonds to the oxygen of Gly175, the nitrogen of Gly180, the oxygen of Phe243 at the C-terminal end of strand β D and an oxygen of the first phosphate group of NAD⁺ in a tetragonal coordination. Since Gly175 and Gly180 are the first and third residues in the sequence GxGxxG that is found to be conserved amongst NAD⁺ binding proteins, the associated water molecule may perform a role in stabilising the phosphate binding loop

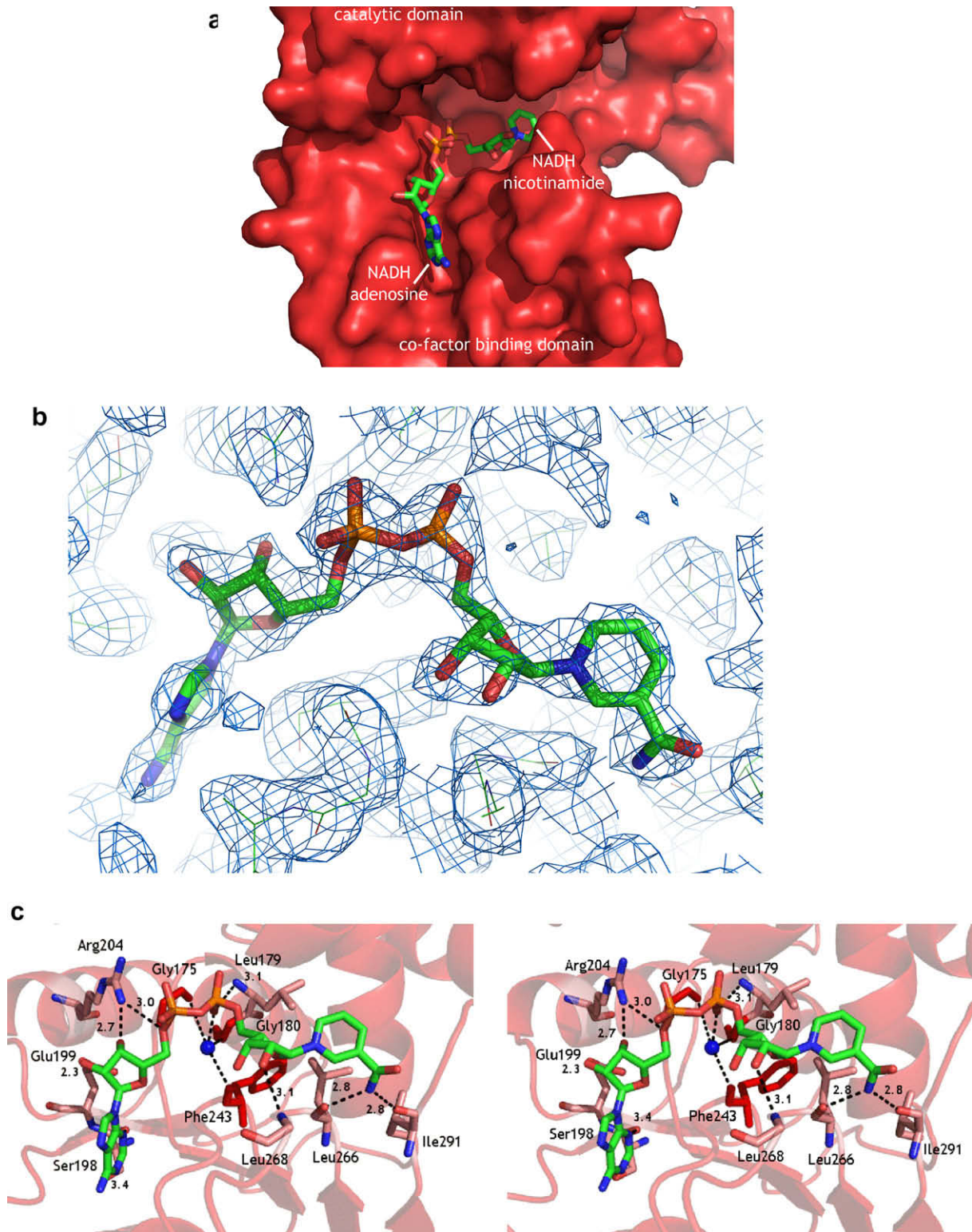


Fig. 6. (a) A surface representation of the NAD⁺ binding cleft between the catalytic and co-factor binding domains. (b) The refined electron density for NAD⁺ in one of the TkTDH monomers. (c) A stereoview showing the extensive hydrogen bonds (dashed lines) made by NAD⁺ with Leu 179, Ser 198, Glu 199, Arg 204, Leu 266, Leu 268 and Ile 291 (residues shown in pink). Many van der Waal contacts are made with other surrounding residues. The water molecule that is conserved in di-nucleotide binding proteins containing the Rossmann fold is also shown. In TkTDH, this water forms four hydrogen bonds to the oxygen of Gly 175, the nitrogen of Gly 180, the oxygen of Phe 243 and an oxygen of the first phosphate group of NAD⁺ (residues shown in red). (For interpretation of colour mentioned in this figure legend the reader is referred to the web version of the article.)

formed by this motif and have an inherent role in the structure of the Rossmann fold. It is interesting to note that di-nucleotides have huge hydrogen bonding potential with NAD⁺ containing 22 polar

oxygen and nitrogen atoms. On average NAD⁺ forms around 16 hydrogen bonds with the protein (Bottoms et al., 2002) and in the case of TkTDH seven are formed with residues and a further

eight with water molecules. This illustrates how important these bridging waters may be as a component of di-nucleotide recognition and binding.

3.6. Complex formation

TDH is the first enzyme in a two-step metabolic pathway that converts threonine to glycine by oxidising L-threonine to the unstable intermediate 2-amino-3-ketobutyrate. With the participation of CoA as a co-factor, the product is acted on by the second enzyme in the degradation pathway, 2-amino-3-ketobutyrate CoA ligase (KBL). The products of this final reaction are glycine and acetyl-CoA. The reactions catalysed by TDH and KBL have been shown to be coupled, both *in vitro* and *in vivo* (Marcus and Dekker, 1993), which is probably due to the highly reactive nature of the intermediate - under aqueous conditions it undergoes spontaneous decarboxylation to form aminoacetone and CO₂. Gel-filtration has been used to demonstrate a physical interaction between the two enzymes and along with fluorescence experiments these findings indicate that two dimers of KBL associate with one tetramer of TDH (Tressel et al., 1986a).

Since the three-dimensional structure of *E. coli* KBL is known (Schmidt et al., 2001) we used the 3D structure of TDH (reported herein) to model the putative interaction between the two enzymes by various docking analyses. The active sites of KBL are approximately 24 Å apart in the dimer. This corresponds well with the active sites in TDH of monomers A and B (or C and D), which are approximately 28 Å apart. One side of the KBL dimer, where

the active sites are located, has a marked depression that appears to be complimentary to the generally convex surface of the TDH tetramer on the sides where the active sites of dimers A and B (or C and D) are exposed. This indeed suggests that a symmetric complex could be formed by the two enzymes to shield and transfer the unstable intermediate by channelling it between them. A complex could form with one KBL dimer binding to the AB dimer of TDH and a second KBL dimer binding to the CD dimer on the opposite face of the TDH tetramer, as shown in Fig. 7. An approximate rigid-body model of the complex has been made by docking the two proteins by the use of AutoDock (Morris et al., 1998) which confirmed the complimentary concave/convex docking arrangement. As a further step to introduce some flexibility into the amino acids of the interface, the docking was repeated using HADDOCK2.0 (de Vries et al., 2007) with the residues around the central binding interface allowed to move and used as a bias to pull the two surfaces together. The resulting 200 solutions were grouped into eight clusters. The best scoring cluster contained 24% of the solutions with an average backbone rmsd of 0.9 ± 0.4 Å from the best scoring solution that had a Haddock score of -52.9 kcal/mol. For the best model, it appears that a dimer of KBL could open slightly, like a pair of jaws, to fit up against the central 12-stranded β -sheet of each TDH dimer in the tetramer.

The KBL enzyme from *E. coli* has 41% sequence identity with that from *T. kodakaraensis*, similar to the level of identity between the TDHs from the two organisms, which is 43%. The SWISS-MODEL server (Arnold et al., 2006) was used to model the structure of KBL from *T. kodakaraensis* and the electrostatic potentials

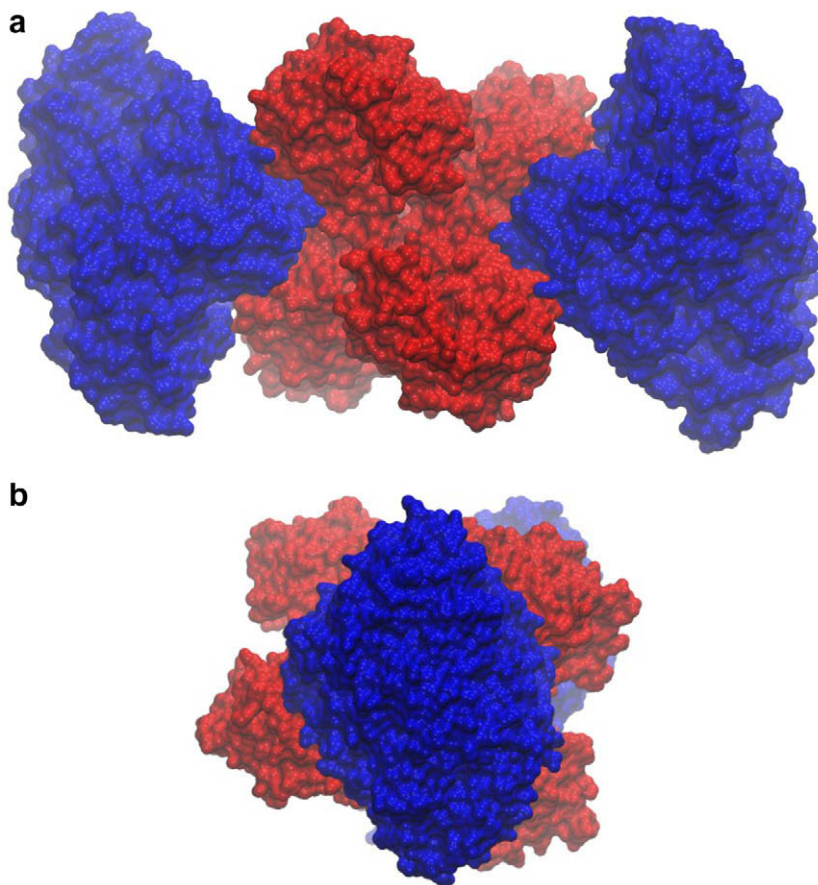


Fig. 7. Two dimers of KBL have been docked with one tetramer of TkdTH, showing their proposed complex formation. Each of the two KBL dimers can dock with a dimer of TkdTH at a relative angle of approximately 45°, allowing them to fit onto opposite faces of the TDH tetramer. This brings the respective active sites into close contact (approximately 30–35 Å from one another). TDH is shown in red and KBL in blue. This putative complex is shown from the active site end of TDH in (a) and a perpendicular view is shown in (b). The product of TDH would be largely shielded from solvent in its passage to the KBL active site. (For interpretation of colour mentioned in this figure legend the reader is referred to the web version of the article.)

calculated, showing a large central region of positive charges on the face of the enzyme thought to bind TDH. An electrostatics model of TkTDH bound to NAD⁺ showed a partial negatively charged surface at the face where it is thought KBL binds, suggesting that electrostatic interactions may also play a role in the complex formation between TDH and KBL. The putative model we have obtained satisfies the charge complementarity of both surfaces and positions the KBL and TDH active sites approximately 30–35 Å apart suggesting the unstable intermediate can pass from one enzyme to the other during turnover.

4. Discussion

The crystal structure of the l-threonine dehydrogenase from *T. kodakaraensis* shows that each monomer of this tetrameric enzyme comprises a catalytic domain and a NAD⁺-binding Rossmann fold domain. In all four monomers the co-enzyme NAD⁺ was present at the active site which resides in a large cleft between the two domains. The enzyme has significant structural similarity with alcohol dehydrogenases, exhibiting the same overall fold of the monomer and assembly of the tetramer, which involves an extended twelve-stranded β -sheet formed by the association of pairs of monomers.

The intriguing finding that each monomer of the enzyme possessed a well-defined NAD⁺ in spite of it being absent from the purification and crystallisation buffers, suggests that the enzyme has a high affinity for the co-factor which is held by extensive contacts with the enzyme, many being mediated by water molecules. Docking the TDH and KBL structures has given much insight into the multi-enzyme complex that they form and the structural nature of substrate channelling in the catabolism of threonine by these two enzymes. It appears that a dimer of KBL could dock with the central 12-stranded β -sheet of each TDH dimer in the tetramer. One side of the KBL dimer, where the active sites are located, has a marked depression that matches the convex surface of the TDH tetramer where the active sites are exposed, both in terms of shape and charge complementarity.

In the putative docked complex, each active site of TDH is approximately 35 Å from the closest KBL active site. The formation of this complex creates a large polar interface between the two enzymes with sufficient cavities and tunnels through which the product of one enzyme could diffuse to the active site of the other and largely avoid contact with bulk solvent. In the putative complex the active site cleft region of TDH forms many contacts with a loop region between Glu170 and His178 of KBL. This loop connects the end of one helix (α 6) with the N-terminal end of a β -strand (β 12) in the PLP-binding domain (Schmidt et al., 2001). This loop is at the outer reaches of the concave side of the KBL dimer and appears to be conserved in homologues suggesting that its putative role in complex formation might be testable by site-directed mutagenesis. Other regions of KBL that would appear to be important in complex formation include parts of the PLP-binding domain that form the inner regions of the 'cup' on the concave side of KBL including the loop connecting α 4 and β 10 along with that connecting α 5 with β 11. The interface between TDH and KBL appears to have limited but sufficient access to solvent to allow the binding of new substrate molecules or the release of products without dissociation of the two enzymes and the same could apply to the binding and release of the NAD⁺ co-enzyme.

Acknowledgements

We gratefully acknowledge the BBSRC for a studentship to A.B. and the ESRF (Grenoble, France) for beam time and travel support.

We thank Drs. A. Coker and P.T. Erskine for assistance with data collection.

References

- Adams, P.D., Grosse-Kunstleve, R.W., Hung, L.W., Ioerger, T.R., McCoy, A.J., Moriarty, N.W., Read, R.J., Sacchettini, J.C., Sauter, N.K., Terwilliger, T.C., 2002. PHENIX: building new software for automated crystallographic structure determination. *Acta Crystallogr. D* 58, 1948–1954.
- Aoyama, Y., Motokawa, Y., 1981. l-threonine dehydrogenase of chicken liver. Purification, characterization, and physiological significance. *J. Biol. Chem.* 256, 12367–12373.
- Arnold, K., Bordoli, L., Kopp, J., Schwede, T., 2006. The SWISS-MODEL workspace: a web-based environment for protein structure homology modelling. *Bioinformatics* 22, 195–201.
- Aronson, B.D., Somerville, R.L., Epperly, B.R., Dekker, E.E., 1989. The primary structure of *E. coli* l-threonine dehydrogenase. *J. Biol. Chem.* 264, 5226–5232.
- Balleve, O., Cadenhead, A., Calder, A.G., Rees, W.D., Lobley, G.E., Fuller, M.F., Garlick, P.J., 1990. Quantitative partition of threonine oxidation in pigs: effect of dietary threonine. *Am. J. Physiol. Endocrinol. Metab.* 259, E483–E491.
- Balleve, O., Houlier, M.L., Prugnaud, J., Bayle, G., Bercovici, D., Seve, B., Arnal, M., 1991. Altered partition of threonine metabolism in pigs by protein-free feeding or starvation. *Am. J. Physiol. Endocrinol. Metab.* 261, E748–E757.
- Barton, G.J., 1993. ALSCRIPT: a tool to format multiple sequence alignments. *Protein Eng.* 6, 37–40.
- Bashir, Q., Rashid, N., Jamil, F., Imanaka, T., Akhtar, M., 2009. Highly thermostable l-threonine dehydrogenase from the hyperthermophilic archaeon *Thermococcus kodakaraensis*. *J. Biochem.* 146, 95–102.
- Bird, M.I., Nunn, P.B., 1983. Metabolic homeostasis of l-threonine in the normally-fed rat. Importance of liver threonine dehydrogenase activity. *Biochem. J.* 214, 687–694.
- Bogin, O., Peretz, M., Burstein, Y., 1997. *Thermoanaerobacter brockii* alcohol dehydrogenase: characterization of the active site metal and its ligand amino acids. *Protein Sci.* 6, 450–458.
- Bottoms, C.A., Smith, P.E., Tanner, J.J., 2002. A structurally conserved water molecule in Rossmann dinucleotide-binding domains. *Protein Sci.* 11, 2125–2137.
- Bowyer, A., Mikolajek, H., Wright, J.N., Coker, A., Erskine, P.T., Cooper, J.B., Bashir, Q., Rashid, N., Jamil, F., Akhtar, M., 2008. Crystallization and preliminary X-ray diffraction analysis of l-threonine dehydrogenase (TDH) from the hyperthermophilic archaeon *Thermococcus kodakaraensis*. *Acta Crystallogr. F* 64, 828–830.
- Boylan, S.A., Dekker, E.E., 1981. l-threonine dehydrogenase. Purification and properties of the homogeneous enzyme from *Escherichia coli* K-12. *J. Biol. Chem.* 256, 1809–1815.
- Brunger, A.T., Adams, P.D., Clore, G.M., DeLano, W.L., Gros, P., Grosse-Kunstleve, R.W., 1998. Crystallography and NMR system: a new software suite for macromolecular structure determination. *Acta Crystallogr. D* 54, 905–921.
- Brunger, A.T., 2007. Version 1.2 of the crystallography and NMR system. *Nat. Protocols* 2, 2728–2733.
- CCP4, 1994. The CCP4 Suite: programs for protein crystallography. *Acta Crystallogr. D* 50, 760–763.
- Dale, R.A., 1978. Catabolism of threonine in mammals by coupling of l-threonine 3-dehydrogenase with 2-amino-3-oxobutyrate-CoA ligase. *Biochim. Biophys. Acta* 544, 496–503.
- Daura, X., Antes, I., van Gunsteren, W.F., Thiel, W., Mark, A.E., 1999. The effect of motional averaging on the calculation of NMR-derived structural properties. *Proteins* 36, 542–555.
- Davis, A.J., Austic, R.E., 1997. Dietary protein and amino acid levels alter threonine dehydrogenase activity in hepatic mitochondria of *Gallus domesticus*. *J. Nutr.* 127, 738–744.
- DeLano, W.L., 2002. The PyMOL Molecular Graphics System. DeLano Scientific, San Carlos, CA, USA. Available from: <<http://www.pymol.org>>.
- de Vries, S.J., van Dijk, A.D.J., Krzeminski, M., van Dijk, M., Thureau, A., Hsu, V., Wassenaar, T., Bonvin, A.M.J.J., 2007. HADDOCK versus HADDOCK: new features and performance of HADDOCK2.0 on the CAPRI targets. *Proteins Struct. Funct. Bioinf.* 69, 726–733.
- Edgar, A.J., 2002a. Molecular cloning and tissue distribution of mammalian l-threonine 3-dehydrogenases. *BMC Biochem.* 3, 19.
- Edgar, A., 2002b. The human l-threonine 3-dehydrogenase gene is an expressed pseudogene. *BMC Genet.* 3, 18.
- Edgar, A., 2005. Mice have a transcribed l-threonine aldolase/GLY1 gene, but the human GLY1 gene is a non-processed pseudogene. *BMC Genomics* 6, 32.
- Emsley, P., Cowtan, K., 2007. Coot: model-building tools for molecular graphics. *Acta Crystallogr. D* 60, 2126–2132.
- Esposito, L., Sica, F., Raia, C.A., Giordano, A., Rossi, M., Mazzarella, L., Zagari, A., 2002. Crystal structure of the alcohol dehydrogenase from the hyperthermophilic archaeon *Sulfolobus solfataricus* at 1.85 Å resolution. *J. Mol. Biol.* 318, 463–477.
- Evans, P.R., 2006. Scaling and assessment of data quality. *Acta Crystallogr. D* 62, 72–82.
- Hammer, V.A., Rogers, Q.R., Freedland, R.A., 1996. Threonine is catabolized by l-threonine 3-dehydrogenase and threonine dehydratase in hepatocytes from domestic cats (*Felis domestica*). *J. Nutr.* 126, 2218–2226.
- Higashi, N., Tanimoto, K., Nishioka, M., Ishikawa, K., Taya, M., 2008. Investigating a catalytic mechanism of hyperthermophilic l-threonine dehydrogenase from *Pyrococcus horikoshii*. *J. Biochem.* 144, 77–85.

- Ishikawa, K., Higashi, N., Nakamura, T., Matsuura, T., Nakagawa, A., 2007. The first crystal structure of L-threonine dehydrogenase. *J. Mol. Biol.* 366, 857–867.
- Itoh, T., 2003. Taxonomy of non-methanogenic hyperthermophilic and related thermophilic archaea. *J. Biosci. Bioeng.* 96, 203–212.
- Jelokova, J.S., Karlsson, C., Estonius, M., Jornvall, H., Hoog, J., 1994. Features of structural zinc in mammalian alcohol dehydrogenase. *Eur. J. Biochem.* 225, 1015–1019.
- Kao, Y.C., Davis, L., 1994. Purification and structural characterization of porcine L-threonine dehydrogenase. *Protein Expr. Purif.* 5, 423–431.
- Kleywegt, G.J., Jones, T.A., 1996. xdlMAPMAN and xdlDATAMAN—programs for reformatting, analysis and manipulation of biomacromolecular electron-density maps and reflection data sets. *Acta Crystallogr. D52*, 826–828.
- Korkhin, Y., Kalb, G., Peretz, M., Bogin, O., Burstein, Y., Frolow, F., 1998. NADP-dependent bacterial alcohol dehydrogenases: crystal structure, cofactor-binding and cofactor specificity of the ADHs of *Clostridium beijerinckii* and *Thermoanaerobacter brockii*. *J. Mol. Biol.* 278, 967–981.
- Laver, W.G., Neuberger, A., Scott, J.J., 1959. Alpha-amino-beta-keto acids. Part II. Rates of decarboxylation of free acids and the behaviour of derivatives on titration. *J. Chem. Soc.*, 1483–1491.
- LeBrun, L.A., Park, D.H., Ramaswamy, S., Plapp, B.V., 2004. Participation of histidine-51 in catalysis by horse liver alcohol dehydrogenase. *Biochemistry* 43, 3014–3026.
- Leskovic, V., Trivic, S., Latkovska, M., 1976. State and accessibility of zinc in yeast alcohol dehydrogenase. *Biochem. J.* 155, 155–161.
- Leslie, A.G.W., 2006. The integration of macromolecular diffraction data. *Acta Crystallogr. D62*, 48–57.
- Marcus, J.P., Dekker, E.E., 1993. Threonine formation via the coupled activity of 2-amino-3-ketobutyrate coenzyme A lyase and threonine dehydrogenase. *J. Bacteriol.* 175, 6505–6511.
- Morikawa, M., Izawa, Y., Rashid, N., Hoaki, T., Imanaka, T., 1994. Purification and characterization of a thermostable thiol protease from a newly isolated hyperthermophilic *Pyrococcus* sp.. *Appl. Environ. Microbiol.* 60, 4559–4566.
- Morris, G.M., Goodsell, D.S., Halliday, R.S., Huey, R., Hart, W.E., Belew, R.K., Olson, A.J., 1998. Automated docking using a Lamarckian genetic algorithm and an empirical binding free energy function. *J. Comput. Chem.* 19, 1639–1662.
- Murzin, A.G., Brenner, S.E., Hubbard, T., Chothia, C., 1995. A structural classification of proteins database for the investigation of sequences and structures. *J. Mol. Biol.* 247, 536–540.
- Potter, R., Kapoor, V., Newman, E.B., 1977. Role of threonine dehydrogenase in *E. coli* threonine degradation. *J. Bacteriol.* 132, 385–391.
- Qian, B., Raman, S., Das, R., Bradley, P., McCoy, A.J., Read, R.J., Baker, D., 2007. High-resolution structure prediction and the crystallographic phase problem. *Nature* 450, 259–264.
- Ramaswamy, S., Park, D.H., Plapp, B.V., 1999. Substitutions in a flexible loop of horse liver alcohol dehydrogenase hinder the conformational change and unmask hydrogen transfer. *Biochemistry* 38, 13951–13959.
- Ray, M., Ray, S., 1984. L-threonine dehydrogenase from goat liver. *J. Biol. Chem.* 260, 5913–5918.
- Rossmann, M.G., Liljas, A., 1974. Recognition of structural domains in globular proteins. *J. Mol. Biol.* 85, 177–181.
- Roth, J.R., Lawrence, J.G., Bobik, T.A., 1996. Cobalamin (coenzyme B₁₂): synthesis and biological significance. *Ann. Rev. Microbiol.* 50, 137–181.
- Schmidt, A., Sivaraman, J., Li, Y., Larocque, R., Barbosa, J.A., Smith, C., Matte, A., Schrag, J.D., Cygler, M., 2001. Three-dimensional structure of 2-amino-3-ketobutyrate CoA ligase from *Escherichia coli* complexed with a PLP-substrate intermediate: inferred reaction mechanism. *Biochemistry* 40, 5151–5160.
- Smith, R.M., Martell, A.E., 1976. *Critical Stability Constants*. Plenum Press, New York.
- Sulzenbacher, G., Alvarez, K., Van Den Heuvel, R.H., Versluis, C., Spinelli, S., Campanacci, V., Valencia, C., Cambillau, C., Eklund, H., Tegoni, M., 2004. Crystal structure of *E. coli* alcohol dehydrogenase YqhD: evidence of a covalently modified NADP coenzyme. *J. Mol. Biol.* 342, 489–502.
- Tressel, T., Thompson, R., Zieske, L.R., Menendez, M.I., Davis, L., 1986a. Interaction between L-threonine dehydrogenase and aminoacetone synthetase and mechanism of aminoacetone production. *J. Biol. Chem.* 261, 16428–16437.
- Tressel, T., Thompson, R., Zieske, L.R., Menendez, M.I., Davis, L., 1986b. Interaction between L-threonine dehydrogenase and aminoacetone synthetase and mechanism of aminoacetone production. *J. Biol. Chem.* 261, 16428–16437.
- Wagner, M., Andreessen, J.R., 1995. Purification and characterization of threonine dehydrogenase from *Clostridium sticklandii*. *Arch. Microbiol.* 163, 286–290.
- Yeung, Y.G., 1986. L-threonine aldolase is not a genuine enzyme in rat liver. *Biochem. J.* 237, 187–190.